



Adropin promotes testicular functions by modulating redox homeostasis in adult mouse

Shashank Tripathi¹ · Shweta Maurya¹ · Ajit Singh ¹

Received: 16 April 2024 / Accepted: 4 June 2024

© The Author(s), under exclusive licence to Springer Science+Business Media, LLC, part of Springer Nature 2024

Abstract

Purpose Adropin is an emerging metabolic hormone that has a role in regulating energy homeostasis. The present study aimed to explore the impact of adropin on redox homeostasis and its possible role in testicular functions in adult mouse testis.

Methods Western blot, flow-cytometry, and TUNEL assay were performed to explore the impact of intra-testicular treatment of adropin (0.5 µg/testis) on testicular functions of adult mice. Hormonal assay was done by ELISA. Further, antioxidant enzyme activities were measured.

Results Adropin treatment significantly increased the sperm count and testicular testosterone by increasing the expression of GPR19 and steroidogenic proteins. Also, adropin treatment reduced the oxidative/nitrosative stress by facilitating the translocation of NRF2 and inhibiting NF-κB into the nucleus of germ cells. Enhanced nuclear translocation of NRF2 leads to elevated biosynthesis of antioxidant enzymes, evident by increased HO-1, SOD, and catalase activity that ultimately resulted into declined LPO levels in adropin-treated mice testes. Furthermore, adropin decreased nuclear translocation of NF-κB in germ cells, that resulted into decreased NO production leading to decreased nitrosative stress. Adropin/GPR19 signaling significantly increased its differentiation, proliferation, and survival of germ cells by elevating the expression of PCNA and declining caspase 3, cleaved caspase 3 expression, Bax/Bcl2 ratio, and TUNEL-positive cells. FACS analysis revealed that adropin treatment enhances overall turnover of testicular cells leading to rise in production of advanced germ cells, notably spermatids.

Conclusion The present study indicated that adropin improves testicular steroidogenesis, spermatogenesis via modulating redox potential and could be a promising target for treating testicular dysfunctions.

Keywords Adropin · GPR19 · Redox homeostasis · Steroidogenesis · Spermatogenesis

Introduction

The maintenance of normal cellular functions is critically dependent on balance between reactive oxygen species (ROS) generation and elimination. The prevalence of oxidative stress occurs when the generation of ROS surpasses the protective mechanisms of antioxidants [1]. Oxidative stress has been associated with the development of several illnesses, including obesity, metabolic syndrome, diabetes, cardiovascular disease, cancers, and infertility [2–4].

Recently, reproductive research has focused extensively on the significance of ROS and associated oxidative stress in male infertility. Conversely, various studies supported the physiological function of ROS and regulated redox balance in male reproduction [5, 6]. The significance of ROS as intracellular signaling molecules cannot be overstated; nevertheless, their overproduction can pose a threat to antioxidant defense system, which may lead to testicular dysfunction [7, 8]. Also, ROS can exert a negative influence on hormonal LH signaling through the modification of oxidant-sensitive MAPK pathways and obstruction of mitochondrial cholesterol transport [9]. Of note, decreased efficacy of antioxidant systems contributes to development of environment with high oxidative stress, which ultimately suppresses Leydig cell steroidogenesis [10, 11]. Therefore, an adequate testicular redox state is vital to maintain normal progression of testicular steroidogenesis and spermatogenesis. Various

✉ Ajit Singh
ajitsinghrepro@gmail.com

¹ Department of Zoology, Institute of Science, Banaras Hindu University, Varanasi 221005, India

cytokines like adiponectin, Nesfatin-1 are reported to improve testicular functions by maintaining redox homeostasis [12, 13].

Adropin, a polypeptide of 76 amino acids, is coded by *Enho* gene, and was initially found in mouse liver and brain by Kumar et al. [14]. The amino acid sequence of adropin in humans is identical to mice, which play a vital role in regulating energy homeostasis [14, 15]. Adropin achieves its diverse roles through interaction with the G-protein coupled receptor 19 [16]. Previous studies have extensively established that GPR19 is a putative receptor for adropin. Thapa et al. [17] showed that the action of adropin on PDK4 in cardiac cells is blocked by genetic depletion of GPR19 or the inhibition of downstream signaling via p44/42 MAP-Kinase [17]. Another study found that suppressing the GPR19 gene in the brain reduced the ability of adropin to regulate drinking caused by water deprivation [18]. Rao et al. [19] further verify that adropin is an intrinsic ligand for GPR19 [19]. Several studies have established a link between adropin and metabolic ailments. Epidemiological studies indicate a substantial decrease in serum adropin levels in metabolic disorders including obesity, diabetes and heart disease [20]. Notably, lack of adropin in mice resulted into enhanced adipose tissue levels and impaired glucose metabolism. Also, adropin administration to diet-induced obese mice improved glucose metabolism and insulin signaling [21]. Further, overexpression or administration of adropin upregulated NRF2 and NRF2-associated antioxidant enzyme expression [19]. Consistent with these findings, the deletion or treatment of adropin worsened or improved the progression of NASH and hepatic injury via the CBP-NRF2-mediated antioxidant response pathway in rodents [22]. The induction of antioxidant responses is significantly attributed to NRF2 which involved in redox homeostasis [23]. It belongs to leucine zipper transcription factor family, is a crucial regulator of several antioxidant enzymes, such as NAD(P)H quinone oxidoreductase-1 (NQO1), heme oxygenase-1 (HO-1) and glutathione S-transferase [24, 25]. The cellular responses to oxidative stress and inflammation are co-regulated by NRF2 and NF- κ B pathways [26]. NF- κ B is also a multifaceted protein complex composed of transcription factors that modulate gene expression, thereby impacting innate and adaptive immunity, inflammation, oxidative stress responses, and B-cell maturation [27].

However, only few reports are available regarding the role of adropin in reproduction. Adropin has been shown to hasten the pubertal changes and regulates the formation of the corpus luteum in adult mouse ovary [28, 29]. While in testis, adropin was found to be expressed in the Leydig cells and it increases insulin stimulated steroidogenesis. Our previous study suggested that adropin binds to its receptor (GPR19) in an autocrine/paracrine mode and it leads to

activation of MAP-Kinase pathway which promotes steroidogenesis, proliferation and survival of the testicular cells [30]. Our another finding suggested that adropin is expressed throughout the postnatal development and promotes pubertal transition in mice testis [31]. Considering the close association between male reproductive functions and a balanced redox state that significantly contributes to testicular activities, our hypothesis states that adropin can potentially manifest as a protective agent against ROS. Thus, the aim of this investigation was to examine whether adropin can trigger an antioxidant response that aids in the removal of ROS and protects against oxidative stress induced testicular dysfunction.

Materials and methods

Animals

All the studies were received approval from the Institutional Animal Ethical Committee (BHU/ DoZ/ IAEC/2019-20/ 032) of Banaras Hindu University. The mice were housed under standard laboratory condition and provided with food pellet and tap water *ad libitum*. This study employed reproductively active (15 weeks old) male mice of Swiss strain.

Peptide and chemicals

The highly conserved peptide sequence H-CHSR SADV DSLSESSPNSSPGPCPEKAPPPQKPSHEGSYLLQP-OH, which corresponds to Adropin (34–76), was purchased from NovoPro Biosciences Inc. in Shanghai, China. The validation of the adropin antibody was done in the mouse testis using immunoblotting.

Adropin treatment: in vivo study

16 reproductively active male mice were randomly divided into two groups ($n = 8$ /group). The vehicle control (VC) group was treated with Milli-Q water, whereas the adropin (ADR) group was treated with 0.5 μ g/testis adropin. The dose and duration of adropin treatment were selected according to prior study with slight change [32]. The rationale behind selecting 0.5 μ g/testis adropin dose was based on our previous study [31], in which we gave 0.5 μ g adropin to the pre-pubertal mouse and found a very promising and potent effect on pubertal transition. Based on this, we selected this low dose of adropin for the treatment. We administered a bilateral intratesticular treatment of adropin to mice after 6 h of fasting. The adropin treatment was given for duration of 6 h. After that, mice were euthanized under a mild anesthesia dose. The testis was

Table 1 List of antibodies that are used for Western blot and immunofluorescence study

S.No.	Antibody	Host species	Source	Catalog no.	Dilutions
1	GPR19	Rabbit; Polyclonal	G Biosciences	ITA5843	1:500 (WB)
2	StAR	Rabbit; Polyclonal	Santa Cruz Biotechnology	SC 25806	1:1000 (WB)
3	P450-SCC	Rabbit; Polyclonal	Cell Signaling Technology, Inc.	14217	1:1000 (WB)
4	3 β -HSD	Rabbit; Polyclonal	Thermo Fisher Scientific Inc.	PA5-27791	1:800 (WB)
5	17 β -HSD	Rabbit; Polyclonal	Thermo Fisher Scientific Inc.	PA5-28065	1:800 (WB)
6	PCNA	Rabbit; Polyclonal	Thermo Fisher Scientific Inc.	PA1-38424	1:500 (WB)
7	HO-1	Rabbit; Polyclonal	Cell Signaling Technology, Inc.	70081	1:1000 (WB)
8	NRF2	Rabbit; Polyclonal	Thermo Fisher Scientific Inc.	710574	1:500 (WB) 1:200 (IF)
9	NF- κ B	Rabbit; Polyclonal	Thermo Fisher Scientific Inc.	710048	1:500 (WB) 1:200 (IF)
10	Bcl 2	Rabbit; Polyclonal	Santa Cruz Biotechnology	(N-20, sc-492)	1:500 (WB)
11	Bax	Rabbit; Polyclonal	Cell Signaling Technology, Inc.	2772	1:800 (WB)
12	Caspase 3	Rabbit; Polyclonal	BIOSS	BS-0081R	1:800 (WB)
13	β -Actin	Mouse; Monoclonal HRP-tagged	Sigma Aldrich	A3854	1: 50000 (WB)
14	Rabbit IgG	Goat	GeNei	1140380011730	1:4000 (WB)
15	Alexa Fluor 488 Rabbit IgG	Goat; Polyclonal	Abcam	ab150077	1:300 (IF)

List of antibodies used for western blot and immunofluorescence

GPR19 G Protein- coupled receptor 19, *StAR* Steroidogenic acute regulatory protein, *P450-SCC* Cytochrome P450 Side chain cleavage, *3 β -HSD* 3 beta- hydroxysteroid dehydrogenase, *17 β -HSD* 17 beta- hydroxysteroid dehydrogenase, *PCNA* proliferating cell nuclear antigen, *Bcl2* B-cell lymphoma 2 protein, *Bax* Bcl-2-associated X protein, *Caspase 3* cysteine-aspartic acid protease 3, *PVDF* polyvinylidene fluoride, *ECL* enhanced chemiluminescence, *DPX* Dibutylphthalate polystyrene xylene, *NRF-2* nuclear factor erythroid 2- related factor 2, *HO-1* Heme oxygenase 1, *NF- κ B* nuclear factor- kappa B

excised in a random manner, cleaned, and one side of the testis was kept at -20°C for immunoblotting and hormonal assays. While the other side of the testis was fixed for immunohistochemical examinations.

Sperm count

The cauda epididymis was removed after sacrifice and utilized for sperm counting. The quantification of sperm was conducted as described by past study [33]. The cauda epididymis was put in petri dish containing 0.5 ml of 0.9% normal saline and finely chopped. Sperm suspension was utilized for quantification in a haemocytometer (Fein-Optik Jena, Germany).

Testosterone (T) assay

ELISA kit was purchased from DiaMetra, Italy (Code: DKO0002). Briefly, 25 μl of the standards, control or serum samples were taken and enzyme conjugate solution (100 μl) was added, followed by 1-hour incubation at 37°C . After aspiration, wells were washed thrice with wash solution. Subsequently, 100 μl of a tetramethyl benzidine (TMB) was poured into wells and incubated at room temperature for 15 min. Furthermore, upon the addition of 100 μl of the stop

solution (0.15 M sulfuric acid), the optical density (OD) was determined at 450 nm using a microplate reader (BioRad).

Western blotting

20% (w/v) homogenate of a testicular sample was obtained using a suspension buffer containing 0.1 M NaCl, 0.01 M Tris, 0.001 M EDTA, with a pH of 8.0, 1 g/ml aprotinin and 100 g/ml PMSF. Protein isolation and immunoblotting was conducted as described by earlier study [34]. 80 μg of protein quantified by Bradford method [32] was run onto 12% SDS-PAGE and were electrophoretically transferred to a polyvinylidene difluoride (PVDF) membrane (Millipore India Pvt. Ltd.) at 50 volts, 4°C for overnight. The membranes were blocked using 5% fat-free dried milk prepared in phosphate-buffered saline (PBS- 0.1 M, pH 7.4, NaH_2PO_4 –16 mM, Na_2HPO_4 64 mM, NaCl 154 mM, 0.02 Tween 20) for 1 h, followed by 3-hour incubation at room temperature with primary antibodies (dilutions in Table 1). Thereafter, membranes were rinsed and incubated with HRP-tagged secondary antibody for 90 min. After thrice washing with PBST, the signal was identified and blot was developed using an enhanced chemiluminescence (ECL) detection system (BioRad, USA). Densitometric evaluation of blots was performed by computer-aided image analysis

software (Image J 1.38x, NIH, USA). Data was represented by the integrated density value \pm SEM. The western blot bands were normalized with β -actin.

Evaluation of antioxidant enzyme activities

The enzyme activity of superoxide dismutase (SOD), catalase (CAT), lipid peroxidation (LPO), and nitric oxide (NO) were quantified in the testes. The testes sample were pooled and a homogenate (10% weight/volume) was made in chilled phosphate-buffered saline (0.01 M, pH 7.6). Homogenate was centrifuged at $12000 \times g$ at $4^\circ C$ for 30 min, and supernatant was taken out. Testicular protein was estimated by the Bradford methodology [35].

SOD activity

SOD activity was evaluated as described earlier [36]. 100 μ l of tissue supernatant was mixed with 1.4 ml of reaction mixture, comprised of 1.1 ml PBS (50 mM) at pH 7.6, 80 μ l L-Methionine (20 mM), 80 μ l hydroxylamine hydrochloride (10 mM), 40 μ l Triton-x-100 (1% v/v), and incubated for 5 min at $37^\circ C$. Subsequently, 80 μ l Riboflavin (50 μ M) was poured into each sample under red light conditions and placed in illuminated lamp box for 10 min. Lastly, 1 ml freshly prepared Griess reagent [1% sulfanilamide, 5% orthophosphoric acid, and 0.1% N-(1-naphthyl) ethylenediamine dihydrochloride] was added. Absorbance was measured at 543 nm on multimode microplate reader (Biotek Instruments, USA). Enzyme activity was determined as units (U)/milligram of proteins.

CAT activity

CAT activity was determined using the approach described earlier [37]. 1 ml supernatant was mixed with solution containing 4 ml hydrogen peroxide of 0.8 M, and 5 ml PBS of 0.01 M, followed by 1-minute incubation. Subsequently, 1 ml fraction of above mixture was taken out and 2 ml acidic $K_2Cr_2O_7$ was added. Final mixture was incubated for 10 min at $95^\circ C$. After cooling, absorbance was recorded at 570 nm using multimode microplate reader (Biotek Instruments, USA). The CAT activity was quantified as the rate of H_2O_2 consumption/minute/milligram of protein.

LPO assay

LPO was evaluated using as explained earlier [38]. 0.2 ml supernatant was mixed with 3.3 ml of mixture containing thiobarbituric acid (TBA) reagent [8% sodium dodecyl sulfate (0.2 ml), 20% acetic acid (1.5 ml; pH 3.5), 0.8% TBA (1.5 ml), and 0.8% butylated hydroxyl toluene (0.1 ml)] and incubated for 1 h at $95^\circ C$. After cooling,

reaction mixture was centrifuged at $500 \times g$ for 10 min at $4^\circ C$. The supernatant consisting of malonaldehyde (MDA)-TBA by-product was evaluated at 532 nm using a multimode microplate reader (Biotek Instruments, USA).

Estimation of NO level

Concentration of NO in the testes was determined as described earlier [39], with a little modification of using potassium nitrate (KNO_3) instead of sodium nitrate ($NaNO_3$). Simply, 10% sample homogenate was treated with ethanol to remove proteins, then centrifuged at $10,000 \times g$ for 15 min to separate the supernatant. 100 μ l of graded standard KNO_3 solution and testicular supernatant were separately taken in wells of microtitre plate. Then, 100 μ l VCL₃ solution (0.8% VCL₃ in 1 M HCL) was added to each well. The Griess reagent (50 μ l 0.1% NEDD in distilled water and 50 μ l 2% sulfanilamide in 5% HCL) was rapidly added followed by 45 min incubation at $37^\circ C$. Absorbance was measured at 540 nm. A standard curve was plotted with absorbance values against different concentrations of KNO_3 . The total nitrate-nitrite concentration in testicular samples was determined by interpolating using standard curve.

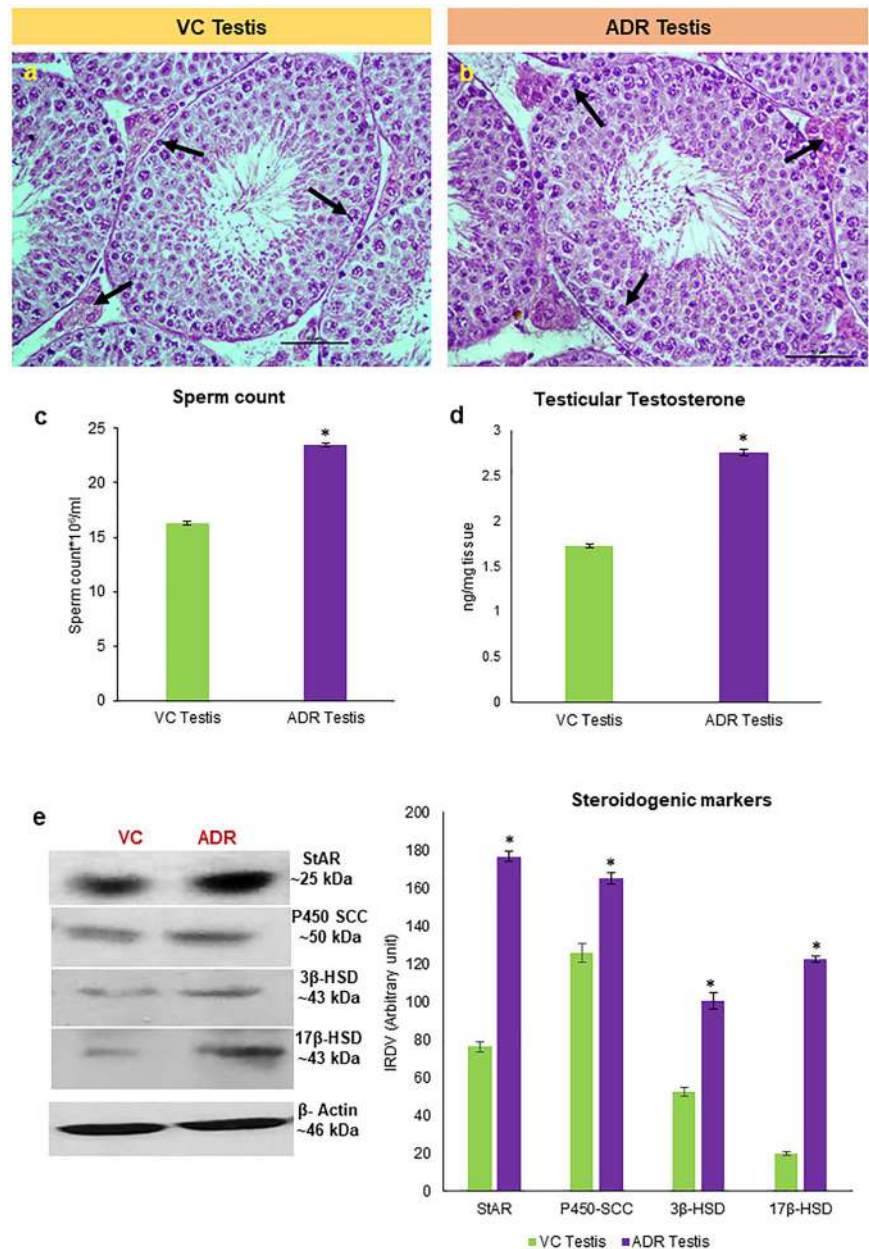
Histological analysis

Testes preserved in Bouin's solution were dehydrated using ascending grades of alcohol, treated with xylene for clearing, and then embedded in paraffin wax. The 6 μ m sections of testes spread on poly L-lysine coated slides. Furthermore, these slides were undergone haematoxylin-eosin and immunofluorescence staining.

Immunofluorescence (IF) detection of NRF-2 and NF- κ B

The testicular sections were deparaffinised with xylene, hydrated in decreasing concentrations of alcohol, and rinsed with 0.1 M PBS (pH 7.4). The antigen retrieval was performed by heating the sections at 750 W in 10 mM citrate buffer solution (pH 6.0) for 10 min. The sections were rinsed thrice with 0.1 M PBS for 5 min each and endogenous peroxidase activity was blocked with 3% H_2O_2 in methanol for 20 min. After washing with 0.1 M PBS, the sections were treated with blocking serum for 2 h, followed by primary antibody (Table 1) incubation for overnight. Subsequently, the sections were rinsed thrice with 0.1 M PBS for 10 min each, and incubated with Alexa Fluor 488 goat anti-rabbit secondary antibody at $25^\circ C$ in dark for 2 h. The slides were rinsed again with 0.1 M PBS, mounted in DABCO, and viewed with a laser scanning super-resolution microscope (Leica, Germany).

Fig. 1 Representative images of adult mice testes (hematoxylin-eosin stained) showing no histological changes after the intra-testicular treatment of adropin (0.5 $\mu\text{g}/\text{testis}$). **a** Testis of VC mice; **b** testis of ADR mice. Testicular sections showing well organized seminiferous tubules (ST) along with normal spermatogonia (Sg) and Leydig cell (LC) morphology. **c** Change in the number of sperm count. **d** Changes in levels of testicular testosterone. **e** Representative western blots and densitometric analysis of steroidogenic markers (StAR, P450-SCC, 3β -HSD, 17β -HSD) in ADR group (dose: 0.5 $\mu\text{g}/\text{testis}$) compared to VC group. IRDV integrated relative density value. Values are represented as mean \pm SEM. Superscript (*) is significantly different ($P < 0.05$) in the dose versus control



Terminal deoxynucleotidyl transferase dUTP nick end labeling (TUNEL) assay

The TUNEL kit (catalog no. E-CK-A331, Elabscience Biotechnology Inc., Texas, USA) was utilized to detect apoptosis inside the histological sections. After depaffinization, rehydration, sections were blocked in 3% H_2O_2 in methanol for 20 min. After rinsing thrice with PBS, sections were subjected to TdT enzyme reaction cocktail (40 ml TdT equilibrium buffer, 5 ml Biotin-dUTP, and 5 ml TdT enzyme) in a moist dark chamber for an hour at 37 $^\circ\text{C}$. Furthermore, sections were rinsed thrice with PBS and incubated with a streptavidin-HRP cocktail for 30 min at 37 $^\circ\text{C}$ in a dark moist chamber. After washing, sections were incubated with the chromogenic

substances 3,3'-Diaminobenzidine (DAB) for 5 min. Eventually, the sections were washed with PBS, counterstained with haematoxylin, dehydrated using graded ethanol, cleared in xylene, mounted in DPX, and photographed (Nikon, Tokyo, Japan). The quantitation of TUNEL-positive cells was performed by calculating the mean TUNEL-positive cells at ten randomly selected seminiferous tubular areas.

Flow cytometry

According to Katoh et al., flow cytometry of testicular tissue was used to assess the impact of adropin on the development of different germ cell types [40]. Testis was chopped using a scissor after removing tunica albuginea in a chilled nutrient

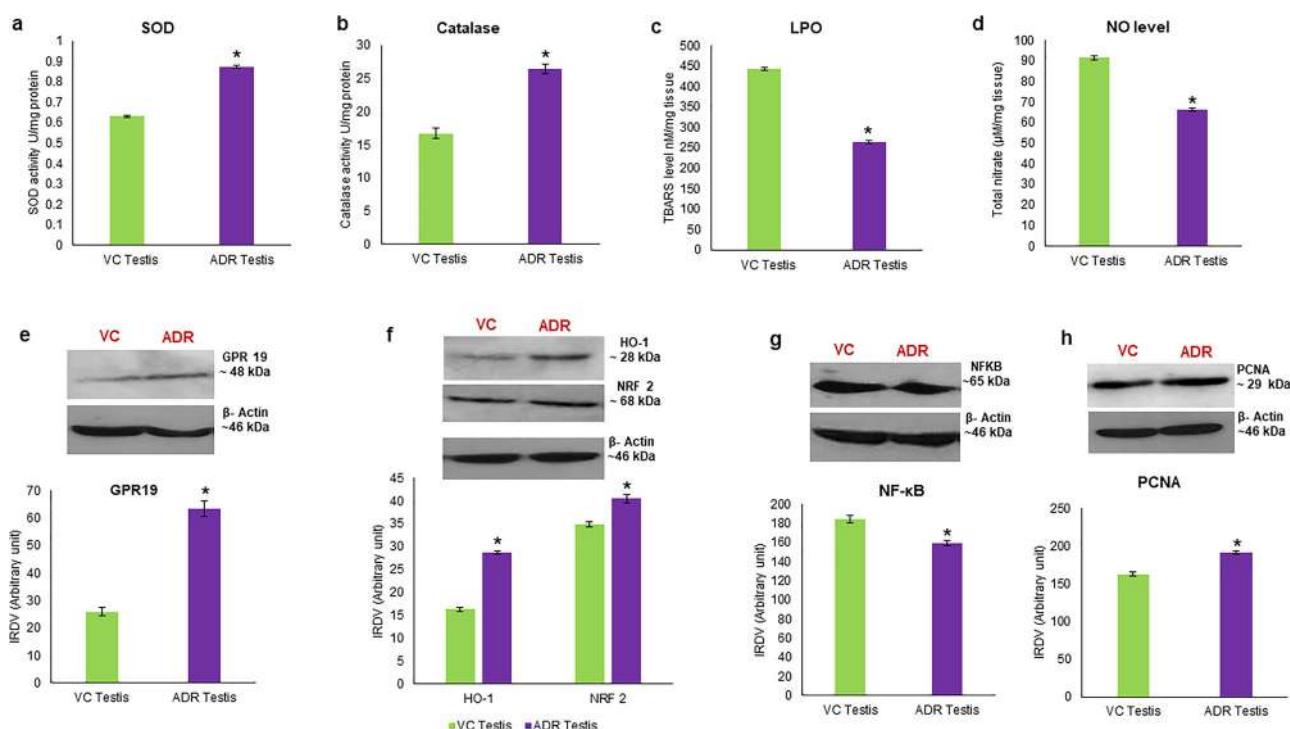


Fig. 2 Effect of bilateral intra-testicular treatment of adropin (0.5 μg/testis) on testicular antioxidant status (a) superoxide dismutase (SOD) activity, (b) catalase activity, (c) lipid peroxidation (LPO) level, and (d) nitric oxide (NO) level in adult mice. Representative immunoblots and densitometric analysis of testicular (e) GPR19, (f) HO-1 & NRF2

proteins, (g) NF-κB, (h) PCNA in adult VC and ADR mice. Data are expressed as mean ± SEM. A bar with a (*) superscript indicates a statistically significant ($P < 0.05$) difference between the mean values of VC and ADR group. VC vehicle control, ADR adropin-treated group

medium (Dulbecco's modified Eagle media). Subsequently, the tissue was immersed in a nutrient medium with 0.25% Type IA collagenase (Sigma, St. Louis, USA) for 30 min at 32.5 °C. Next, the cell suspension was filtered by 40 μm nylon mesh filter (SPL Lifesciences, USA) to remove any residual tissue debris and get single cell suspension. Subsequently, the suspension was centrifuged at 300 xg for 5 min and pellet was washed twice using nutritional media. One aliquot of each cell suspension was treated with 0.2% trypan blue to assess the viability of the suspension. The cells were fixed using 70% chilled methanol and stored at -20 °C for 24 h. Then, the cell samples were treated with 0.25% concentration of RNase (Bangalore Genei, India). Two consecutive wash with PBS were done before to staining with a Propidium Iodide solution (50 mg/ml in PBS) (PI; Sigma, St. Louis, USA). This staining process was performed in the dark at 4 °C for 30 min. Based on the total amount of DNA that each cell contained, a flow cytometer (CytoFLEX LX, Beckman Coulter, USA) was used to count the cells.

Statistical analysis

The statistical analyses were conducted using SPSS version 16 software (SPSS Inc, IBM, Chicago, IL, USA). An unpaired t-test was used to examine the significance of the mean values of VC and ADR mice. Data were

presented as mean ± SEM, whereas densitometric data were shown as the mean of integrated relative density value (IRDV) ± SEM. The data were regarded statistically significant if $P < 0.05$.

Results

Effect of intra-testicular treatment of adropin on testicular histoarchitecture, sperm count and testosterone biosynthesis of adult mice

Intra-testicular treatment of adropin caused no major histological alterations. Testicular sections of adropin treated (0.5 μg/testis) mice showed well organized seminiferous tubules with various stages of developing germ cells (Fig. 1a, b). However, adropin treatment resulted into a significant ($P < 0.05$) increase in the number of sperm count and testicular T levels in ADR compared to VC group (Fig. 1c, d).

Effect of intra-testicular treatment of adropin on the expression of steroidogenic markers and GPR19 proteins in the adult mice

The intra-testicular treatment of adropin (0.5 μg/testis) caused significant increase ($P < 0.05$) in the expression of

StAR, P450-SCC, 3 β -HSD and 17 β -HSD protein in ADR compared to VC group (Fig. 1e). Further, adropin treatment resulted into significant elevation ($P < 0.05$) in the expression of GPR19 protein compared to VC group (Fig. 2e).

Effect of intra-testicular treatment of adropin on antioxidant enzymes activity, LPO, and NO levels in the adult mice

Biochemical estimation of antioxidant enzymes (SOD & CAT) were found to be significantly increased ($P < 0.05$) in the ADR (0.5 μ g/testis) compared to VC group (Fig. 2a, b). Furthermore, LPO and NO levels demonstrated significant decrease ($P < 0.05$) ADR compared to VC group (Fig. 2c, d).

Effect of intra-testicular treatment of adropin on the expression of HO-1, NRF2, NF- κ B in adult mice

The effect of intra-testicular treatment of adropin (0.5 μ g/testis) on the expression of HO-1, NRF2, NF- κ B was evaluated by western blot. The result showed significantly increased expression of HO-1 and NRF2 proteins (Fig. 2f) while NF- κ B protein was significantly declined ($P < 0.05$) in ADR compared to VC group (Fig. 2g).

Effect of intra-testicular treatment of adropin on the immunofluorescence detection of NRF2 and NF- κ B in adult mice

The effect of intra-testicular treatment of adropin (0.5 μ g/testis) on the localization of NRF2 and NF- κ B in the testis was evaluated by immunofluorescence study. NF- κ B localization was found more in cytoplasmic compartment than nuclear compartment in the germ cells of ADR compared to VC testis (Fig. 3). While, the NRF2 protein was found more in nuclear compartment than cytoplasmic compartment in the germ cells of ADR compared to VC testis (Fig. 4).

Effect of intra-testicular treatment of adropin on the expression of PCNA (cell proliferation marker), Bax, Bcl2, Caspase 3 & cleaved caspase 3 (apoptotic) markers, and TUNEL positive cells in adult mice

Western blot revealed the significantly increased ($P < 0.05$) expression of PCNA protein in ADR compared to VC group (Fig. 2h). Further, adropin treatment significantly upregulated ($P < 0.05$) the expression of Bcl2 protein whereas significantly downregulated ($P < 0.05$) the expression of Bax, caspase 3 and cleaved caspase 3 proteins in ADR compared to VC group (Fig. 5a, b). Also, significant decrease ($P < 0.05$) was noted in Bax/Bcl-2

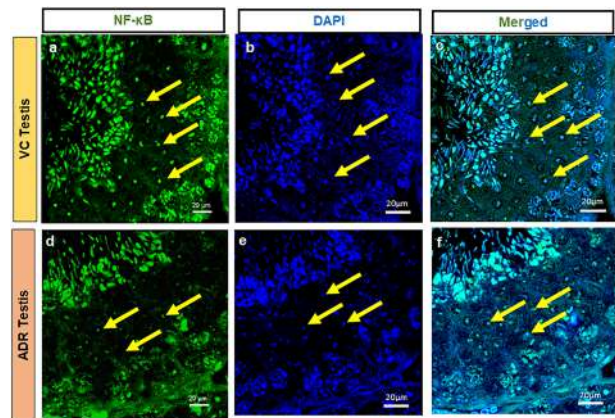


Fig. 3 Representative immunofluorescence image of NF- κ B (a, d), nuclear staining with DAPI (b, e) and merged image of NF- κ B protein with DAPI (c, f) in the paraffin-embedded testicular sections of adult mouse treated with adropin (0.5 μ g/testis). Note- Yellow arrow indicates nuclear compartment of germ cells

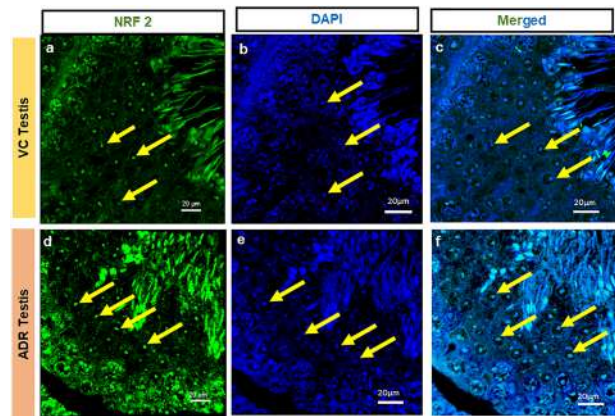


Fig. 4 Representative immunofluorescence image of NRF2 (a, d), nuclear staining with DAPI (b, e) and merged image of NRF2 protein with DAPI (c, f) in the paraffin-embedded testicular sections of adult mouse treated with adropin (0.5 μ g/testis). Note- Yellow arrow indicates nuclear compartment of germ cells

ratio (Fig. 5c). Further, decreased TUNEL positive cells were observed in ADR compared to VC testis (Fig. 5d, e–g). Also, significant decline was noted in the mean TUNEL positive cell number in ADR compared to VC testis (Fig. 5h).

Effect of adropin treatment on testicular germ cell kinetics

Adult mice treated with adropin showed significant increase ($P < 0.05$) in the number of 1C and 4C phase cells while significant decrease ($P < 0.05$) in 2C phase cells in ADR compared to VC group (Fig. 6c). Further, ratio of 1C:2C and 4C:2C was found to be significantly elevated ($P < 0.05$), whereas 1C:4C ratio was significantly declined ($P < 0.05$) in ADR compared to VC group (Fig. 6d).

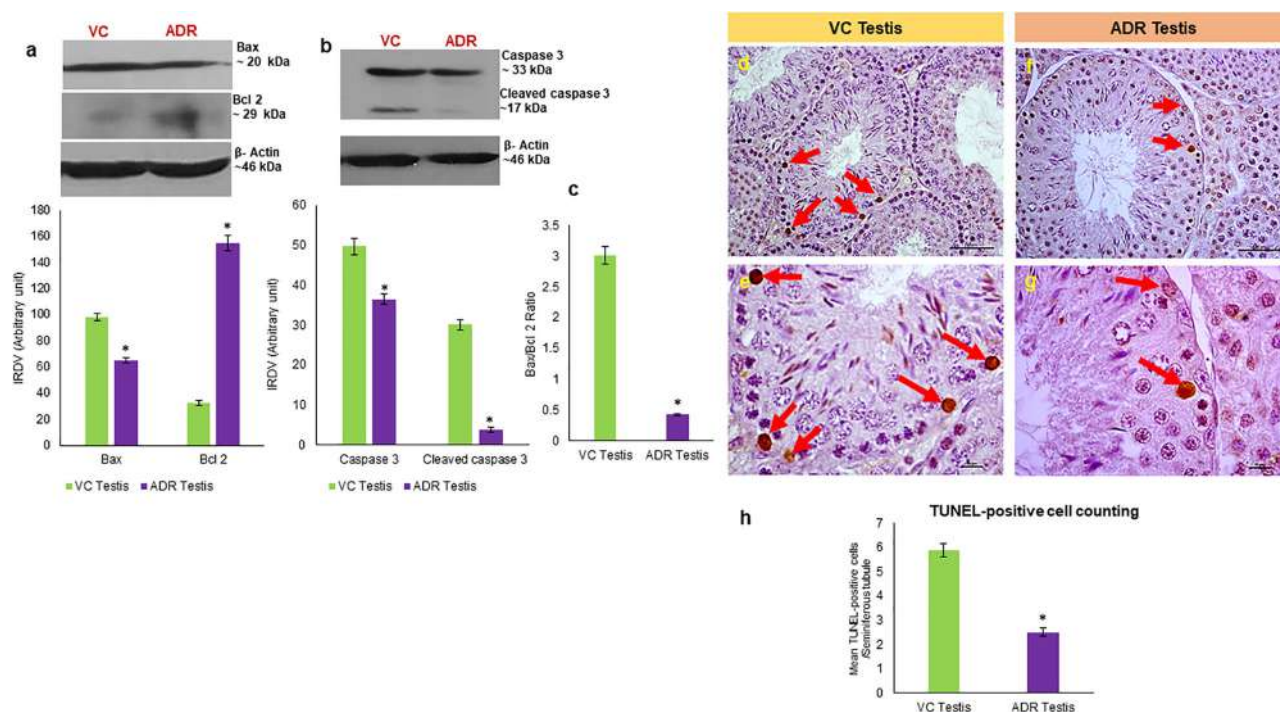


Fig. 5 Representative immunoblots and densitometric analysis of (a) Bax and Bcl2, (b) Caspase 3 and cleaved caspase 3 proteins in VC and ADR group. c The bar graph shows the Bax/Bcl2 ratio (in %) in the testis of adropin-treated adult mice. Representative images showing TUNEL-positive cells in the testicular histology of adult mice treated with adropin (0.5 $\mu\text{g}/\text{testis}$). d, e VC testis, (f, g) ADR testis (0.5 $\mu\text{g}/\text{testis}$). h Representative histogram showing mean TUNEL-positive

cells in the testis of adropin treated adult mouse (0.5 $\mu\text{g}/\text{testis}$) as compared to VC testis. d f at $\times 40$ and (e, g) at $100\times$ magnification. Note- Red arrow indicates apoptotic spermatogonia. Data are expressed as IRDV \pm SEM, analyzed by unpaired t-test. A bar with a (*) superscript indicates a significant ($p < 0.05$) difference between the mean values of VC and ADR groups. VC vehicle control, ADR adropin-treated (0.5 $\mu\text{g}/\text{testis}$) group

Discussion

This study was carried out to investigate the direct role of adropin on gonadal functions in adult mouse testis. In our previous study, we reported the presence of adropin and GPR19 mRNA and protein in adult mice testes [30, 31]. Adropin was found to be mainly localized in Leydig cells while its receptor GPR19 expression was observed in Leydig cells as well as pachytene, primary and secondary spermatocytes [30, 31]. Based on these findings we hypothesized that adropin may regulate testicular function in adult mice in an autocrine/paracrine manner. To find out the direct role, intra testicular treatment of adropin was given to adult mice. Histological study demonstrates no notable alterations in adropin treated mice testes and were characterized by the presence of properly arranged seminiferous tubules containing all tubular cells, including spermatogonia, spermatocytes, Sertoli cells, spermatids and interstitial cells (Leydig cells).

Further we examined the effect of intra-testicular treatment of adropin on testicular steroidogenesis and spermatogenesis. Adropin treatment resulted into significantly increased expression of GPR19, StAR, P450-SCC, 3β -HSD, 17β -HSD, along with increased testosterone level

and sperm count. StAR and CYP11A1 plays crucial role in steroidogenesis, acting as rate-limiting factors responsible for transporting cholesterol from outer to inner mitochondrial membrane and converting cholesterol to pregnenolone, respectively [41]. The 3β -HSD facilitates conversion of pregnenolone to progesterone and dehydroepiandrosterone to androstenedione by catalysis. Conversely, 17β -HSD is accountable for transformation of androstenedione into testosterone [41]. Testosterone is essential hormone that facilitates various processes critical for spermatogenesis such as sustenance of BTB, promotion of meiotic completion, attachment of elongated spermatids to Sertoli cells, and release of sperm [42]. So, these findings clearly indicate that adropin via GPR19 promotes the expression of StAR, P450-SCC, 3β -HSD, 17β -HSD resulted in increased testosterone synthesis that may enhance sperm production.

The testes are highly vulnerable to oxidative stress due to presence of ROS generating system and unsaturated fatty acids [43]. In present study, adropin treatment significantly declined LPO level while significant increase was observed in NRF2, HO-1, expression and antioxidant enzymes (SOD, Catalase) activity. Also IF study demonstrated increased nuclear translocation of NRF2 in germ cells of adropin treated mice testis. NRF2 is key

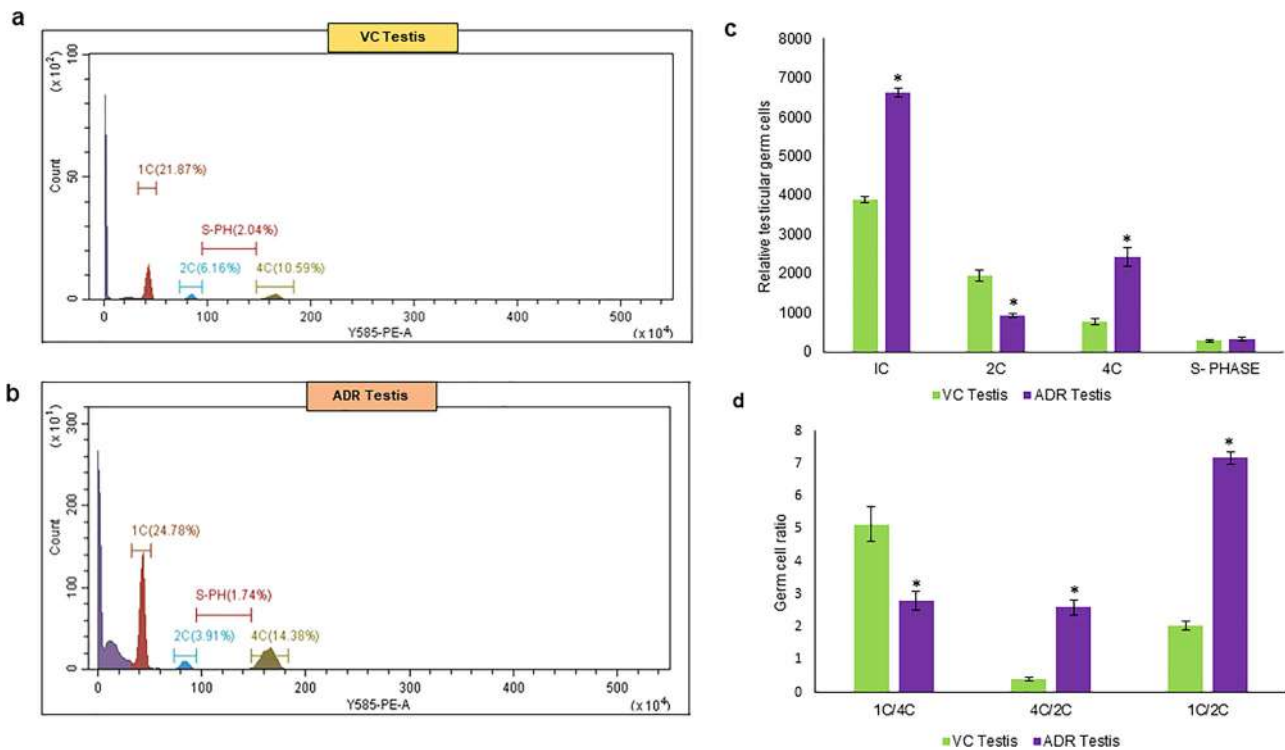


Fig. 6 Representative histogram showing DNA content distribution of testicular germ cells in adult mice. **a** VC testis, **b** ADR testis (0.5 μ g/testis). **c**, **d** Effect of adropin on relative percentage of different types

of germ cell population and on germ cell ratio in mice. Values are represented as mean \pm SEM. Values (*) is significantly different ($P < 0.05$) in dose versus control

sensor of oxidative stress and plays vital role in shielding the testis from oxidative stress [44]. Increased oxidative load increases translocation of NRF2 into nucleus where it binds to ARE and promotes the activation of HO-1, SOD and Catalase. SOD neutralizes free radicals by converting superoxide into H_2O_2 and H_2O_2 toxicity is prevented by catalase mediated conversion of H_2O_2 into H_2O [45]. HO-1 plays crucial role in haem degradation resulting in bilirubin synthesis which has antioxidant property [46]. Increased oxidative load has been shown to increase LPO leading to loss of structure and function of plasma membrane [47]. Altogether these findings clearly indicate that adropin promotes translocation of NRF2 in nucleus resulting into increased production of SOD and Catalase, thereby reduces oxidative stress. NF- κ B, a redox sensitive transcription factor, links oxidative stress with inflammation and apoptosis [48]. Increased NO interacts with reactive nitrogen/oxygen species to trigger nitrosative/oxidative stress [49]. Previous study has reported increased ROS promotes activation of NF- κ B by stimulating its translocation from cytoplasm to nucleus [50]. NO level has been found to be elevated in conditions that causes testicular oxidative stress such as cryptorchidism, testicular torsion, and obstructive azoospermia [51–53]. So these finding clearly indicated that adropin decreases nitrosative/oxidative stress by inhibiting translocation of

NF- κ B into the nucleus of germ cells that resulted in decreased NO production.

Previous studies have reported the negative role of male fertilities in various pathophysiological conditions [54]. So, we planned to examine the effect of adropin on testicular germ cell proliferation and apoptosis. Adropin treatment significantly increased cell proliferation (PCNA) and survival markers (Bcl-2) while significant decline was observed in pro-apoptotic proteins (Bax, caspase-3 and active caspase-3). PCNA is marker for proliferation of spermatogonia and spermatocytes in humans and rats [55, 56]. It is involved in DNA synthesis in mitotic cells and detected during late G1 and S phases of growth and proliferation of germ cells in testis [57]. Notably, testicular germ cells express Bcl-2 that exhibits a positive correlation with spermatogenic cycle [58]. Bcl2 also plays crucial role in maintaining integrity of Sertoli cells [59]. Additionally, cells with low Bax/Bcl-2 ratio exhibit reduced sensitivity to apoptotic stimuli compared to cells with high Bax/Bcl-2 ratio [60]. Caspases are group of cysteine proteases which induces apoptosis through their activation cascade. Caspase-3 is the final common executor of apoptosis [61]. These observations indicated that adropin promotes germ cell proliferation but inhibits apoptosis which was further confirmed by TUNEL assay in which we observed reduction in TUNEL positive cells in the ADR testis.

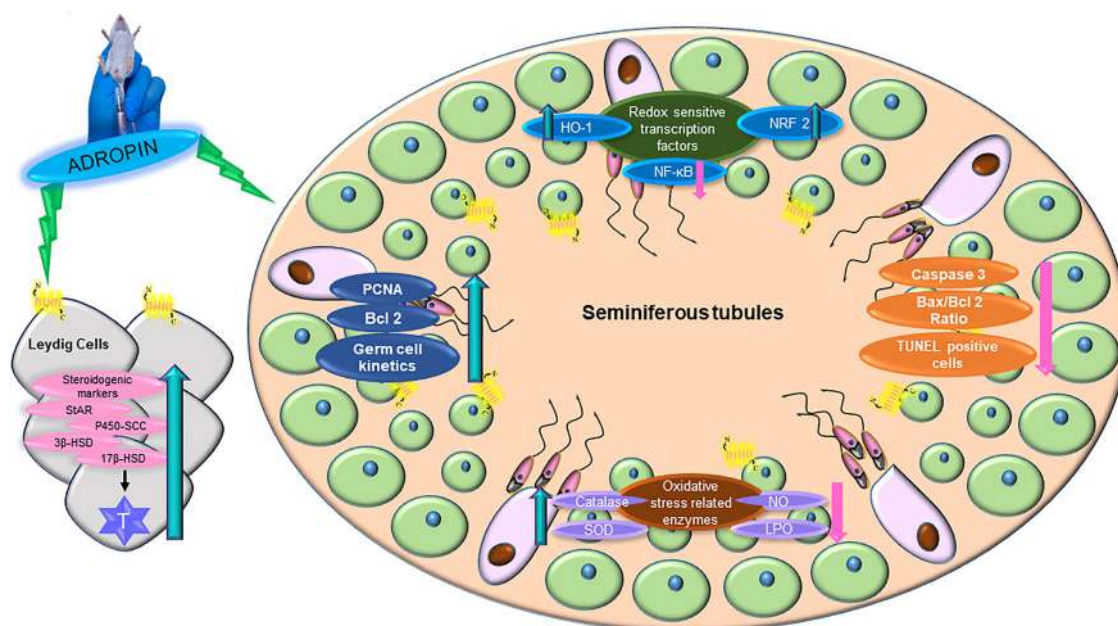


Fig. 7 A schematic diagram shows the possible role of adropin on testicular functions and redox homeostasis in adult mice. Adropin administration elevates testicular testosterone production by increasing the expression of GPR19 and steroidogenic enzymes (StAR, P450SCC, 3 β -HSD, 17 β -HSD). Further, adropin decreases oxidative/nitrosative stress by promoting nuclear translocation of NRF2 and inhibiting NF- κ B translocation in germ cells. Increased nuclear translocation of NRF2 in adropin treated mice results in to increased production of antioxidant enzymes like HO-1, SOD and catalase leading to decreased oxidative stress that is evident by decreased LPO level. Adropin inhibits the nuclear translocation of NF- κ B in the germ

cells resulting in to decreased NO production, suggestive of decreased nitrosative stress. Furthermore, adropin/GPR19 signaling enhances the proliferation, differentiation, and survival of germ cells by upregulating the expression of PCNA (a marker for cell proliferation) and downregulating the expression of caspase3, cleaved caspase 3 protein (a marker for cell apoptosis), the Bax/Bcl2 ratio, and TUNEL-positive cells that results in increased production of advanced germ cells, mainly spermatids. Conclusively, the study indicates that adropin promotes testicular steroidogenesis, spermatogenesis by inhibiting testicular oxidative stress and can be used as a potential therapeutic option for testicular dysfunction

Finally, to examine which germ cell type are most affected by adropin treatment, we performed flow cytometric analysis. The flow cytometry technique is reliable for quantification of various germ cells in testes, on the basis of their DNA content. Spermatogenesis involves multiplication and differentiation of germ cells into successive cell types, each having varying DNA makeup. Flowcytometric assessment demonstrated that adropin treatment results in significant increase in population of 1C (round spermatids), 4C (primary spermatocytes) cells, and a decline in the 2C (spermatogonia) cell population. Reduction in number of 2C phase cells is indicative of acceleration of germ cell differentiation into subsequent cell types [62]. Notably, differences between the treated mice and controls in number of 1C and 2C phase cells show the proportionate surge in 1C and 4C cell population (per 20,000 cells counted) in contrast to other cell types. Also, administration of adropin resulted in significant increase in both 4C:2C and 1C:2C ratio, which serves as indication of its ability to enhance the overall turnover of testicular cells.

In summary, the entire study offers valuable insights into effect of adropin on testicular functions (steroidogenesis and spermatogenesis) and redox homeostasis in adult mice testes. Adropin administration elevates testicular testosterone

production by increasing the expression of GPR19 and steroidogenic enzymes. Adropin also decreases oxidative/nitrosative stress by promoting nuclear translocation of NRF2 and inhibiting NF- κ B translocation in germ cells. Increased nuclear translocation of NRF2 results into increased production of antioxidant enzymes like HO-1, SOD and catalase, resulting into decreased oxidative stress that is evident by decreased LPO level. Adropin inhibits the nuclear translocation of NF- κ B in the germ cells resulting in decreased NO production which is suggestive of decreased nitrosative stress. Additionally, adropin/GPR19 signaling enhances the proliferation, differentiation, and survival of germ cells by upregulating expression of PCNA and downregulating expression of Caspase3, cleaved caspase 3 protein, Bax/Bcl2 ratio, and TUNEL-positive cells. This eventually results in increased production of advanced germ cells, specifically spermatids. Overall, adropin enhances testicular functions and redox potential, which could be utilized as potential therapeutic targets for testicular dysfunctions (Fig. 7).

Acknowledgements S.T. and S.M. highly acknowledge CSIR, New Delhi, for the grant as JRF and SRF. DST-FIST and UGC-CAS

program to the Department of Zoology, BHU, is acknowledged. The authors are thankful to Sophisticated Analytical and Technical Help Institute (SATHI), BHU, India, for providing a laser scanning super-resolution microscope facility and Institute of eminence, BHU for flow-cytometry facility.

Author contributions The experiments were conceptualized and designed by all authors. S.T. and S.M. conducted all the experiments and prepared graphs and figures. All authors analyzed the data. S.T. wrote the manuscript. A.S. reviewed the work and edited the final version of manuscript. All the authors read and agreed to publish the final manuscript.

Funding This work was financially supported by grants from Indian council of medical research (ICMR) (File no. 5/10/FR/54/2020-RBMCH) New Delhi, India and Bridge grant (SRICC/Bridge Grant/2023-24/8135) under Institute of eminence scheme, BHU.

Compliance with ethical standards

Conflict of interest The authors declare no competing interests.

References

1. I. Fridovich, Superoxide dismutases. An adaptation to a paramagnetic gas. *J. Biol. Chem.* **264**(14), 7761–7764 (1989)
2. R. Brigelius-Flohé, M. Maiorino, Glutathione peroxidases. *Biochimica et Biophysica Acta* **1830**(5), 3289–3303 (2013). <https://doi.org/10.1016/j.bbagen.2012.11.020>
3. E. Niedzielska, I. Smaga, M. Gawlik, A. Moniczewski, P. Stan-kowicz, J. Pera, M. Filip, Oxidative stress in neurodegenerative diseases. *Mol. Neurobiol.* **53**(6), 4094–4125 (2016). <https://doi.org/10.1007/s12035-015-9337-5>
4. G. Pizzino, N. Irrera, M. Cucinotta, G. Pallio, F. Mannino, V. Arcoraci, F. Squadrito, D. Altavilla, A. Bitto, Oxidative stress: Harms and benefits for human health. *Oxid. Med. Cell. Longev.* **2017**, 8416763 (2017). <https://doi.org/10.1155/2017/8416763>
5. R.J. Aitken, M. Paterson, H. Fisher, D.W. Buckingham, M. van Duin, Redox regulation of tyrosine phosphorylation in human spermatozoa and its role in the control of human sperm function. *J. Cell Sci.* **108**(Pt 5), 2017–2025 (1995). <https://doi.org/10.1242/jcs.108.5.2017>
6. E. de Lamirande, C. Gagnon, A positive role for the superoxide anion in triggering hyperactivation and capacitation of human spermatozoa. *Int. J. Androl.* **16**(1), 21–25 (1993). <https://doi.org/10.1111/j.1365-2605.1993.tb01148.x>
7. S. Dutta, A. Majzoub, A. Agarwal, Oxidative stress and sperm function: A systematic review on evaluation and management. *Arab J. Urol.* **17**(2), 87–97 (2019). <https://doi.org/10.1080/2090598X.2019.1599624>
8. P. Sabeti, S. Pourmasumi, T. Rahiminia, F. Akyash, A.R. Talebi, Etiologies of sperm oxidative stress. *Int. J. Reprod. Biomed.* **14**(4), 231–240 (2016)
9. T. Diemer, J.A. Allen, K.H. Hales, D.B. Hales, Reactive oxygen disrupts mitochondria in MA-10 tumor Leydig cells and inhibits steroidogenic acute regulatory (StAR) protein and steroidogenesis. *Endocrinology* **144**(7), 2882–2891 (2003). <https://doi.org/10.1210/en.2002-0090>
10. L. Cao, S. Leers-Sucheta, S. Azhar, Aging alters the functional expression of enzymatic and non-enzymatic anti-oxidant defense systems in testicular rat Leydig cells. *J. Steroid Biochem. Mol. Biol.* **88**(1), 61–67 (2004). <https://doi.org/10.1016/j.jsbmb.2003.10.007>
11. H. Chen, A.S. Pechenino, J. Liu, M.C. Beattie, T.R. Brown, B.R. Zirkin, Effect of glutathione depletion on Leydig cell steroidogenesis in young and old brown Norway rats. *Endocrinology* **149**(5), 2612–2619 (2008). <https://doi.org/10.1210/en.2007-1245>
12. M. Choubey, A. Ranjan, P.S. Bora, F. Baltazar, L.J. Martin, A. Krishna, Role of adiponectin as a modulator of testicular function during aging in mice. *Biochimica et Biophys Acta Mol. Basis Dis.* **1865**(2), 413–427 (2019). <https://doi.org/10.1016/j.bbadis.2018.11.019>
13. A. Ranjan, M. Choubey, T. Yada, A. Krishna, Direct effects of neuropeptide nesfatin-1 on testicular spermatogenesis and steroidogenesis of the adult mice. *Gen. Comp. Endocrinol.* **271**, 49–60 (2019). <https://doi.org/10.1016/j.ygcn.2018.10.022>
14. K.G. Kumar, J.L. Trevaskis, D.D. Lam, G.M. Sutton, R.A. Koza, V.N. Chouljenko, K.G. Kousoulas, P.M. Rogers, R.A. Kesterson, M. Thearle, A.W. Ferrante Jr, R.L. Mynatt, T.P. Burriss, J.Z. Dong, H.A. Halem, M.D. Culler, L.K. Heisler, J.M. Stephens, A.A. Butler, Identification of adropin as a secreted factor linking dietary macronutrient intake with energy homeostasis and lipid metabolism. *Cell Metab.* **8**(6), 468–481 (2008). <https://doi.org/10.1016/j.cmet.2008.10.011>
15. A.A. Butler, J. Zhang, C.A. Price, J.R. Stevens, J.L. Graham, K.L. Stanhope, S. King, R.M. Krauss, A.A. Bremer, P.J. Havel, Low plasma adropin concentrations increase risks of weight gain and metabolic dysregulation in response to a high-sugar diet in male nonhuman primates. *J. Biol. Chem.* **294**(25), 9706–9719 (2019). <https://doi.org/10.1074/jbc.RA119.007528>
16. L.M. Stein, G.L. Yosten, W.K. Samson, Adropin acts in brain to inhibit water drinking: potential interaction with the orphan G protein-coupled receptor, GPR19. *Am. J. Physiol. Regulatory Integr. Comp. Physiol.* **310**(6), R476–R480 (2016). <https://doi.org/10.1152/ajpregu.00511.2015>
17. D. Thapa, M.W. Stoner, M. Zhang, B. Xie, J.R. Manning, D. Guimaraes, S. Shiva, M.J. Jurczak, I. Scott, Adropin regulates pyruvate dehydrogenase in cardiac cells via a novel GPCR-MAPK-PDK4 signaling pathway. *Redox Biol.* **18**(Sep 1), 25–32 (2018). <https://doi.org/10.1152/ajpheart.00449.2020>
18. B.A. Mushala, I. Scott, Adropin: a hepatokine modulator of vascular function and cardiac fuel metabolism. *Am. J. Physiol.-Heart Circulatory Physiol.* **320**(1 Jan), H238–H244 (2021). <https://doi.org/10.1016/j.bbamcr.2017.05.001>
19. A. Rao, D.R. Herr, G protein-coupled receptor GPR19 regulates E-cadherin expression and invasion of breast cancer cells. *Biochimica et Biophysica Acta (BBA)-Mol. Cell Res.* **1864**(7 Jul), 1318–1327 (2017). <https://doi.org/10.1016/j.redox.2018.06.003>
20. I.I. Ali, C. D’Souza, J. Singh, E. Adeghate, Adropin’s role in energy homeostasis and metabolic disorders. *Int. J. Mol. Sci.* **23**(15), 8318 (2022). <https://doi.org/10.3390/ijms23158318>
21. K. Ganesh Kumar, J. Zhang, S. Gao, J. Rossi, O.P. McGuinness, H.H. Halem, M.D. Culler, R.L. Mynatt, A.A. Butler, Adropin deficiency is associated with increased adiposity and insulin resistance. *Obes. (Silver Spring, Md.)* **20**(7), 1394–1402 (2012). <https://doi.org/10.1038/oby.2012.31>
22. X. Chen, H. Xue, W. Fang, K. Chen, S. Chen, W. Yang, T. Shen, X. Chen, P. Zhang, W. Ling, Adropin protects against liver injury in nonalcoholic steatohepatitis via the Nrf2 mediated antioxidant capacity. *Redox Biol.* **21**, 101068 (2019). <https://doi.org/10.1016/j.redox.2018.101068>
23. Q. Ma, Role of nrf2 in oxidative stress and toxicity. *Annu. Rev. Pharmacol. Toxicol.* **53**, 401–426 (2013). <https://doi.org/10.1146/annurev-pharmtox-011112-140320>
24. H. Zhao, S. Eguchi, A. Alam, D. Ma, The role of nuclear factor-erythroid 2 related factor 2 (Nrf-2) in the protection against lung

- injury. *Am. J. Physiol. Lung Cell. Mol. Physiol.* **312**(2), L155–L162 (2017). <https://doi.org/10.1152/ajplung.00449.2016>
25. R. Zhang, M. Xu, Y. Wang, F. Xie, G. Zhang, X. Qin, Nrf2-a promising therapeutic target for defending against oxidative stress in stroke. *Mol. Neurobiol.* **54**(8), 6006–6017 (2017). <https://doi.org/10.1007/s12035-016-0111-0>
 26. J.D. Wardyn, A.H. Ponsford, C.M. Sanderson, Dissecting molecular cross-talk between Nrf2 and NF- κ B response pathways. *Biochem Soc. Trans.* **43**(4), 621–626 (2015). <https://doi.org/10.1042/BST20150014>
 27. M.J. Morgan, Z.G. Liu, Crosstalk of reactive oxygen species and NF- κ B signaling. *Cell Res.* **21**(1), 103–115 (2011). <https://doi.org/10.1038/cr.2010.178>
 28. S. Maurya, S. Tripathi, T. Arora, A. Singh, Adropin may regulate corpus luteum formation and its function in adult mouse ovary. *Hormones (Athens, Greece)* **22**(4), 725–739 (2023). <https://doi.org/10.1007/s42000-023-00476-0>
 29. S. Maurya, S. Tripathi, A. Singh, Ontogeny of adropin and its receptor expression during postnatal development and its prognadal role in the ovary of pre-pubertal mouse. *J. Steroid Biochem. Mol. Biol.* **234**, 106404 (2023). <https://doi.org/10.1016/j.jsmb.2023.106404>
 30. S. Tripathi, S. Maurya, A. Singh, Adropin may promote insulin stimulated steroidogenesis and spermatogenesis in adult mice testes. *J. Exp. Zool. Part A Ecol. Integr. Physiol.* **341**(1), 86–98 (2024). <https://doi.org/10.1002/jez.2763>
 31. S. Tripathi, S. Maurya, A. Singh, Adropin, a novel hepatokine: localization and expression during postnatal development and its impact on testicular functions of pre-pubertal mice. *Cell Tissue Res.* **395**(2), 171–187 (2024). <https://doi.org/10.1007/s00441-023-03852-9>
 32. L. Yu, Z. Lu, S. Burchell, D. Nowrangi, A. Manaenko, X. Li, Y. Xu, N. Xu, J. Tang, H. Dai, J.H. Zhang, Adropin preserves the blood-brain barrier through a Notch1/Hes1 pathway after intracerebral hemorrhage in mice. *J. Neurochem* **143**(6), 750–760 (2017). <https://doi.org/10.1111/jnc.14238>
 33. A. Banerjee, A. Singh, P. Srivastava, H. Turner, A. Krishna, Effects of chronic bhang (cannabis) administration on the reproductive system of male mice. *Birth Defects Res. Part B Developmental Reprod. Toxicol.* **92**(3), 195–205 (2011). <https://doi.org/10.1002/bdrb.20295>
 34. S. Maurya, A. Singh, Asprosin modulates testicular functions during ageing in mice. *Gen. Comp. Endocrinol.* **323–324**, 114036 (2022). <https://doi.org/10.1016/j.ygcen.2022.114036>
 35. M.M. Bradford, A rapid and sensitive method for the quantitation of microgram quantities of protein utilizing the principle of protein-dye binding. *Anal. Biochem.* **72**, 248–254 (1976). <https://doi.org/10.1006/abio.1976.9999>
 36. K. Das, L. Samanta, N.B.G. Chainy, A modified spectrophotometric assay of superoxide dismutase using nitrite formation by superoxide radicals. *Ind. J. Biochem Biophys.* **37**, 201–204 (2000)
 37. A.K. Sinha, Colorimetric assay of catalase. *Anal. Biochem.* **47**(2), 389–394 (1972). [https://doi.org/10.1016/0003-2697\(72\)90132-7](https://doi.org/10.1016/0003-2697(72)90132-7)
 38. H. Ohkawa, N. Ohishi, K. Yagi, Reaction of linoleic acid hydroperoxide with thiobarbituric acid. *J. lipid Res.* **19**(8), 1053–1057 (1978)
 39. K.M. Miranda, M.G. Espey, D.A. Wink, A rapid, simple spectrophotometric method for simultaneous detection of nitrate and nitrite. *Nitric Oxide: Biol. Chem.* **5**(1), 62–71 (2001). <https://doi.org/10.1006/niox.2000.0319>
 40. C. Katoh, S. Kitajima, Y. Saga, J. Kanno, I. Horii, T. Inoue, Assessment of quantitative dual-parameter flow cytometric analysis for the evaluation of testicular toxicity using cyclophosphamide- and ethynylestradiol-treated rats. *J. Toxicol. Sci.* **27**(2), 87–96 (2002). <https://doi.org/10.2131/jts.27.87>
 41. W.L. Miller, H.S. Bose, Early steps in steroidogenesis: intracellular cholesterol trafficking. *J. lipid Res.* **52**(12), 2111–2135 (2011). <https://doi.org/10.1194/jlr.R016675>
 42. L.B. Smith, W.H. Walker, The regulation of spermatogenesis by androgens. *Semin. Cell Dev. Biol.* **30**, 2–13 (2014). <https://doi.org/10.1016/j.semcdb.2014.02.012>
 43. R.J. Aitken, S.D. Roman, Antioxidant systems and oxidative stress in the testes. *Oxid. Med. Cell. Longev.* **1**(1), 15–24 (2008). <https://doi.org/10.4161/oxim.1.1.6843>
 44. A. Wajda, J. Łapczuk, M. Grabowska, M. Słojewski, M. Laszczyńska, E. Urasińska, M. Drożdżik, Nuclear factor E2-related factor-2 (Nrf2) expression and regulation in male reproductive tract. *Pharmacol. Rep.* **68**(1), 101–108 (2016). <https://doi.org/10.1016/j.pharep.2015.07.005>
 45. Y. Wang, R. Branicky, A. Noë, S. Hekimi, Superoxide dismutases: Dual roles in controlling ROS damage and regulating ROS signaling. *J. Cell Biol.* **217**(6), 1915–1928 (2018). <https://doi.org/10.1083/jcb.201708007>
 46. S.W. Ryter, R.M. Tyrrell, The heme synthesis and degradation pathways: role in oxidant sensitivity. Heme oxygenase has both pro- and antioxidant properties. *Free Radic. Biol. Med.* **28**(2), 289–309 (2000). [https://doi.org/10.1016/s0891-5849\(99\)00223-3](https://doi.org/10.1016/s0891-5849(99)00223-3)
 47. R.F. Jacob, R.P. Mason, Lipid peroxidation induces cholesterol domain formation in model membranes. *J. Biol. Chem.* **280**(47), 39380–39387 (2005). <https://doi.org/10.1074/jbc.M507587200>
 48. V.U. Nna, A.B. Abu Bakar, A. Ahmad, C.O. Eleazu, M. Mohamed, Oxidative stress, NF- κ B-mediated inflammation and apoptosis in the testes of streptozotocin-induced diabetic rats: Combined protective effects of malaysian propolis and metformin. *Antioxid. (Basel, Switz.)* **8**(10), 465 (2019). <https://doi.org/10.3390/antiox8100465>
 49. J.S. Aprioku, Pharmacology of free radicals and the impact of reactive oxygen species on the testis. *J. Reprod. Infertil.* **14**(4), 158–172 (2013)
 50. Y. Kabe, K. Ando, S. Hirao, M. Yoshida, H. Handa, Redox regulation of NF-kappaB activation: distinct redox regulation between the cytoplasm and the nucleus. *Antioxid. redox Signal.* **7**(3–4), 395–403 (2005). <https://doi.org/10.1089/ars.2005.7.395>
 51. T. Ishikawa, Y. Kondo, K. Goda, M. Fujisawa, Overexpression of endothelial nitric oxide synthase in transgenic mice accelerates testicular germ cell apoptosis induced by experimental cryptorchidism. *J. Androl.* **26**(2), 281–288 (2005). <https://doi.org/10.1002/j.1939-4640.2005.tb01096.x>
 52. K. Shiraiishi, K. Naito, K. Yoshida, Nitric oxide promotes germ cell necrosis in the delayed phase after experimental testicular torsion of rat. *Biol. Reprod.* **65**(2), 514–521 (2001). <https://doi.org/10.1095/biolreprod65.2.514>
 53. M.M. Başar, U. Kisa, D. Tuğlu, E. Yilmaz, H. Başar, O. Çağlayan, E. Batislam, Testicular nitric oxide and thiobarbituric acid reactive substances levels in obstructive azoospermia: a possible role in pathophysiology of infertility. *Mediators Inflamm.* **2006**(3), 27458 (2006). <https://doi.org/10.1155/MI/2006/27458>
 54. A. Agarwal, R.A. Saleh, M.A. Bedaiwy, Role of reactive oxygen species in the pathophysiology of human reproduction. *Fertil. Steril.* **79**(4), 829–843 (2003). [https://doi.org/10.1016/s0015-0282\(02\)04948-8](https://doi.org/10.1016/s0015-0282(02)04948-8)
 55. K. Steger, I. Aleithe, H. Behre, M. Bergmann, The proliferation of spermatogonia in normal and pathological human seminiferous epithelium: an immunohistochemical study using monoclonal antibodies against Ki-67 protein and proliferating cell nuclear antigen. *Mol. Hum. Reprod.* **4**(3), 227–233 (1998). <https://doi.org/10.1093/molehr/4.3.227>
 56. A. Godlewski, W. Bołoz, A. Chilarski, The anti-PCNA reaction in the seminiferous tubule cells of Lewis rat testis. Part II: The unilateral inflammatory effect of Freund's complete adjuvant. *Folia Histochemica et. Cytobiologica* **37**(2), 81–82 (1999)

57. M.B. Mathews, R.M. Bernstein, B.R. Franza Jr, J.I. Garrels, Identity of the proliferating cell nuclear antigen and cyclin. *Nature* **309**(5966), 374–376 (1984). <https://doi.org/10.1038/309374a0>
58. A. Banerjee, S. Anjum, R. Verma, A. Krishna, Alteration in expression of estrogen receptor isoforms alpha and beta, and aromatase in the testis and its relation with changes in nitric oxide during aging in mice. *Steroids* **77**(6), 609–620 (2012). <https://doi.org/10.1016/j.steroids.2012.02.004>
59. A. Giannattasio, G. Angeletti, M. De Rosa, S. Zarrilli, M. Ambrosino, A. Cimmino, C. Coppola, G. Panza, R. Calafiore, A. Colao, O. Abete, G. Lombardi, RNA expression bcl-w, a new related protein Bcl-2 family, and caspase-3 in isolated sertoli cells from pre-pubertal rat testes. *J. Endocrinol Investig.* **25**(7), RC23–RC25 (2002). <https://doi.org/10.1007/BF03345074>
60. H. Perlman, X. Zhang, M.W. Chen, K. Walsh, R. Buttyan, An elevated bax/bcl-2 ratio corresponds with the onset of prostate epithelial cell apoptosis. *Cell Death Differ.* **6**(1), 48–54 (1999). <https://doi.org/10.1038/sj.cdd.4400453>
61. P. Saikumar, Z. Dong, V. Mikhailov, M. Denton, J.M. Weinberg, M.A. Venkatachalam, Apoptosis: definition, mechanisms, and relevance to disease. *Am. J. Med.* **107**(5), 489–506 (1999). [https://doi.org/10.1016/s0002-9343\(99\)00259-4](https://doi.org/10.1016/s0002-9343(99)00259-4)
62. S.K. Patel, S. Singh, S.K. Singh, Standardized extract of *Bacopa monnieri* (CDRI-08): Effect on germ cell dynamics and possible mechanisms of its beneficial action on spermatogenesis and sperm quality in male mice. *Biochem Biophys Res. Commun.* **494**(1-2), 34–41 (2017). <https://doi.org/10.1016/j.bbrc.2017.10.089>

Publisher's note Springer Nature remains neutral with regard to jurisdictional claims in published maps and institutional affiliations.

Springer Nature or its licensor (e.g. a society or other partner) holds exclusive rights to this article under a publishing agreement with the author(s) or other rightsholder(s); author self-archiving of the accepted manuscript version of this article is solely governed by the terms of such publishing agreement and applicable law.